

University of Nebraska - Lincoln

DigitalCommons@University of Nebraska - Lincoln

Publications from USDA-ARS / UNL Faculty

U.S. Department of Agriculture: Agricultural
Research Service, Lincoln, Nebraska

1-21-2016

Hepatic Transcriptomic and Metabolic Responses of Hybrid Striped Bass (*Morone saxatilis* × *Morone chrysops*) to Acute and Chronic Hypoxic Insult

Benjamin H. Beck
USDA, Agricultural Research Service

S. Adam Fuller
USDA, Agricultural Research Service


Chao Li
Auburn University

Bartholomew W. Green
USDA, Agricultural Research Service

Honggang Zhao
Auburn University

See next page for additional authors

Follow this and additional works at: <https://digitalcommons.unl.edu/usdaarsfacpub>

 Part of the [Agriculture Commons](#), and the [Aquaculture and Fisheries Commons](#)

Beck, Benjamin H.; Fuller, S. Adam; Li, Chao; Green, Bartholomew W.; Zhao, Honggang; Rawles, Steven D.; Webster, Carl D.; and Peatman, Eric, "Hepatic Transcriptomic and Metabolic Responses of Hybrid Striped Bass (*Morone saxatilis* × *Morone chrysops*) to Acute and Chronic Hypoxic Insult" (2016). *Publications from USDA-ARS / UNL Faculty*. 2469.
<https://digitalcommons.unl.edu/usdaarsfacpub/2469>

This Article is brought to you for free and open access by the U.S. Department of Agriculture: Agricultural Research Service, Lincoln, Nebraska at DigitalCommons@University of Nebraska - Lincoln. It has been accepted for inclusion in Publications from USDA-ARS / UNL Faculty by an authorized administrator of DigitalCommons@University of Nebraska - Lincoln.

Authors

Benjamin H. Beck, S. Adam Fuller, Chao Li, Bartholomew W. Green, Honggang Zhao, Steven D. Rawles, Carl D. Webster, and Eric Peatman



Hepatic transcriptomic and metabolic responses of hybrid striped bass (*Morone saxatilis* × *Morone chrysops*) to acute and chronic hypoxic insult



Benjamin H. Beck^{a,*}, S. Adam Fuller^b, Chao Li^c, Bartholomew W. Green^b, Honggang Zhao^c, Steven D. Rawles^b, Carl D. Webster^b, Eric Peatman^c

^a United States Department of Agriculture, Agricultural Research Service, Aquatic Animal Health Research Unit, Auburn, AL 36832, USA

^b United States Department of Agriculture, Agricultural Research Service, Stuttgart National Aquaculture Research Center, Stuttgart, AR 72160, USA

^c School of Fisheries, Aquaculture and Aquatic Sciences, Auburn University, Auburn, AL 36849, USA

ARTICLE INFO

Article history:

Received 26 September 2015

Received in revised form 5 January 2016

Accepted 17 January 2016

Available online 21 January 2016

Keywords:

Hypoxia

Morone

Transcriptome

Bass

RNA-seq

Mitochondria

ABSTRACT

Striped bass (*Morone saxatilis*), white bass (*Morone chrysops*), and their hybrid are an important group of fish prized for recreational angling in the United States, and there and abroad as a high-value farmed fish. Regardless of habitat, it is not uncommon for fish of the genus *Morone* to encounter and cope with conditions of scarce oxygen availability. Previously, we determined that hybrid striped bass reared under conditions of chronic hypoxia exhibited reduced feed intake, lower lipid and nutrient retention, and poor growth. To better understand the molecular mechanisms governing these phenotypes, in the present study, we examined the transcriptomic profiles of hepatic tissue in hybrid striped bass exposed to chronic hypoxia (90 days at 25% oxygen saturation) and acute hypoxia (6 h at 25% oxygen saturation). Using high-throughput RNA-seq, we found that over 1400 genes were differentially expressed under disparate oxygen conditions, with the vast majority of transcriptional changes occurring in the acute hypoxia treatment. Gene pathway and bioenergetics analyses revealed hypoxia-mediated perturbation of genes and gene networks related to lipid metabolism, cell death, and changes in hepatic mitochondrial content and cellular respiration. This study offers a more comprehensive view of the temporal and tissue-specific transcriptional changes that occur during hypoxia, and reveals new and shared mechanisms of hypoxia tolerance in teleosts.

Published by Elsevier Inc.

1. Introduction

Hypoxia is a state of oxygen deficiency that is sufficient to cause impairment of organismal function or in extreme cases, death. Hypoxia is becoming an increasingly important environmental concern (Diaz, 2001; Wu et al., 2003), and has received extensive attention in the fisheries sciences, particularly aquaculture. Understanding the tissue-specific and temporal changes in gene expression in fishes exposed to hypoxia could reveal new mechanisms of hypoxia tolerance and shed light on this adaptive response in vertebrates. The role of oxygen in development, physiology, and pathology is an area of long-standing biological interest (Hochachka, 1986). Considerable effort has focused on identifying the molecular links between changes in oxygen tension and its consequences on cellular or organismal function (see Nikinmaa and Rees, 2005 for a review). Most of our understanding about the influence of oxygen on cellular mechanisms and gene expression patterns in animals comes from studies on mammals or well-characterized model organisms, such as zebrafish, *Danio rerio* (Ton et al., 2003),

Caenorhabditis elegans (Jiang et al., 2001), or *Drosophila* (Bacon et al., 1998).

The temperate basses of the genus *Morone* are an economically valuable and ecologically important group of fishes, particularly in the United States, where they are popular as both recreational sportfish and farmed foodfish. Striped bass (*Morone saxatilis*), white bass (*Morone chrysops*) and their hybrid (sunshine bass or Palmetto bass; commonly produced in hatcheries for foodfish and sportfish, respectively) inhabit a range of habitats including rivers, reservoirs, and intensively managed aquaculture impoundments. Irrespective of their environment, at some point in their life cycle fish will likely experience varying degrees of hypoxia, particularly during summer months.

The movements and behavior of inland stocks of striped bass, particularly in reservoirs, have been shown to be tightly linked to dissolved oxygen levels and the presence of thermal refugia. Poor summer habitats featuring a limited availability of cool and oxygenated water can lead to large-scale mortality of striped bass (Coutant, 1985). However, far less is known about the consequences of hypoxia on hybrid striped bass and their habitat preferences under these conditions. In a study monitoring the movements of hybrid striped bass in a reservoir, during summer stratification fish were often found to be restricted to narrow

* Corresponding author.

E-mail address: Benjamin.Beck@ars.usda.gov (B.H. Beck).

bands of water where dissolved oxygen levels were above 2 mg/L (Douglas and Jahn, 1987).

Unlike wild stocks, fish reared in aquaculture production systems such as ponds have few alternatives to avoid hypoxic conditions, often causing fish to move to the surface to pass oxygen-saturated water over their gills (Burggren, 1982) and/or gather around the discharge of the mechanical aerator. In settings of aquaculture, the intensity and duration of hypoxia depend on a variety of factors including fish biomass, feeding rate, phytoplankton blooms, and installed aeration capacity (Green et al., 2015). Previously, we characterized the effects of hypoxia on performance metrics of hybrid striped bass and found that hypoxia led to reduced feed intake, which resulted in lower nutrient retention and growth (Green et al., 2015). However, the precise molecular mechanisms contributing to these disparate phenotypes were unknown. However, recent advancements in genomic resources for striped bass (Li et al., 2014; Reading et al., 2012) and white bass (Li et al., 2014) offer researchers the ability to take a closer look directly at many *Morone* functional pathways that were previously limited to model species. Given the importance of hypoxia on the management and captive rearing of *Morone*, we examine here the transcriptional responses of hybrid striped bass to acute and chronic hypoxia. We highlight unique and shared signatures between hypoxic treatments and the bioenergetic consequences of chronic oxygen deprivation on hepatocellular function. Our findings offer a more comprehensive view of the cellular and molecular consequences of hypoxia and reveal new mechanisms of hypoxia tolerance in teleosts.

2. Methods

This research was conducted at the Harry K. Dupree Stuttgart National Aquaculture Research Center (HKD-SNARC), Agricultural Research Service (ARS), US Department of Agriculture, Stuttgart, Arkansas. Animal care and experimental protocols were approved by the HKD-SNARC Institutional Animal Care and Use Committee and conformed to ARS Policies and Procedures 130.4 and 635.1.

2.1. Experimental animals and systems

The fish used in this study were cohorts of those subjected to hypoxia as previously described by Green et al. (2015). Thirty juvenile hybrid striped bass (HSB; 98.7 ± 12.3 g) in each tank were fed by hand daily as much commercially formulated floating extruded feed (Cargill Animal Nutrition; 45% crude protein, 12% crude fat) as they would consume in 30 min. The study was conducted indoors and consisted of two independent flow-through tank systems each comprised of a 700-L reservoir tank and four 250-L (208-L working volume) treatment tanks (experimental units). Water in each reservoir tank was controlled to maintain a constant dissolved oxygen (DO) concentration in each of the four replicate treatment tanks of 25% (DO25 or chronic hypoxia) or 100% (DO100 or normoxia) of saturation by addition of air, pure oxygen, or pure nitrogen, the latter used to deoxygenate water in the DO25 treatment. A submersible pump in each reservoir (Pondmaster Model 18B, Pentair Aquatic Ecosystems, Apopka, Florida, USA) pumped water to each experimental unit at 10.7 L min^{-1} (hydraulic retention time = 19.5 min). A DO probe (model Type III, Oxyguard International, Birkerød, Denmark; or model DO6200/T, Sensorex, Garden Grove, California, USA) was deployed at 25 cm depth in each treatment tank and reservoir and DO concentration was monitored continuously by datalogger (model CR206, Campbell Scientific Inc., Logan, Utah, USA). A water temperature sensor (model 109, Campbell Scientific Inc., Logan, Utah, USA) was deployed at 25-cm depth in each reservoir tank and one experimental unit per DO concentration to monitor water temperature continuously by datalogger. Dissolved oxygen concentration (% saturation) averaged $23.0 \pm 2.3\%$ and $105.5 \pm 9.5\%$ (mean \pm SD) for the DO25 and DO100 treatment tanks, respectively. The experiment was conducted at ambient water temperature

(22.6 ± 0.6 °C). Fish were held at DO25 and DO100 levels for 90 d after which 9 fish from each treatment were sacrificed and liver samples were collected for RNA-seq. Remaining fish from each tank were removed from their respective treatments using a dip net and immediately placed in the opposite DO saturation DO25 \rightarrow DO100 (restoration of normoxia) and DO100 \rightarrow DO25 (acute hypoxia) for 6 h, after which, 9 fish per treatment were sacrificed and livers collected for RNA-seq.

2.2. RNA extraction, library construction and sequencing

Extractions were performed according to the manufacturer's directions using an RNeasy Plus Universal Mini Kit (Qiagen, Valencia, California). RNA concentration and integrity of each sample were measured on an Agilent 2100 Bioanalyzer using a RNA Nano Bioanalysis chip. For each timepoint, RNA from liver with 3 pooled replicates (each containing liver samples from 3 individuals; totaling 9 fish per treatment) were used for RNA-seq library construction.

RNA-seq library preparation and sequencing were carried out by HudsonAlpha Genomic Services Lab (Huntsville, AL, USA). cDNA libraries were prepared with 2.14–3.25 μg of starting total RNA and using the Illumina TruSeq RNA Sample Preparation Kit (Illumina), as dictated by the TruSeq protocol. The libraries were amplified with 15 cycles of PCR and contained TruSeq indexes within the adaptors, specifically indexes 1–12. Finally, amplified library yields were 30 μL of 19.8–21.4 ng/ μL with an average length of \sim 270 bp, indicating a concentration of 110–140 nM. After KAPA quantitation and dilution, the libraries were clustered 12 per lane and sequenced on an Illumina HiSeq 2000 instrument with 100 bp PE reads.

2.3. De novo assembly of sequencing reads

The de novo assembly was performed on cleaned reads using Trinity (Grabherr et al., 2011). Before assembly, raw reads were trimmed by removing adaptor sequences and ambiguous nucleotides. Reads with quality scores less than 20 and length below 30 bp were all trimmed. The resulting high-quality sequences were used in subsequent assembly. Briefly, the raw reads were assembled into the unique sequences of transcripts in Inchworm via greedy K-mer extension (k-mer 25). After mapping of reads to Inchworm contig bundles, Chrysalis incorporated reads into de Bruijn graphs. Butterfly then processed the individual graphs in parallel, reporting full-length transcripts and paralogous genes.

2.4. Gene annotation and ontology

The assembled contigs were used as queries against the UniProtKB/SwissProt database and the non-redundant (nr) protein database using the BLASTX program. The cutoff E-value was set at $1e-5$ and only the top gene id and name were initially assigned to each contig. Gene ontology (GO) annotation analysis was performed using the nr BLAST results in Blast2GO version 2.6.6, which is an automated tool for the assignment of gene ontology terms (Gotz et al., 2008). The final annotation file was produced after gene-ID mapping, GO term assignment, annotation augmentation and generic GO-Slim process. The annotation result was categorized with respect to Biological Process, Molecular Function, and Cellular Component at level 2.

2.5. Identification of differentially expressed contigs

The high quality reads from each sample were mapped onto the Trinity reference assembly using Bowtie software with default parameters. The RSEM program was then used to estimate the abundance of the transcripts. The total mapped reads number for each transcript was determined, and then normalized to detect FPKM (Fragments Per Kilobase of transcript per Million mapped reads). Differential expression analysis was performed by Bioconductor edge R package. All the samples were

normalized together. Normalization was performed by trimmed mean of M values (TMM). TMM equates the overall expression levels of genes between samples under the assumption that the majority of them are not differentially expressed. Transcripts with absolute fold change values of larger than 1.5 and a FDR p-value < 0.05 were included in the analysis as differentially expressed genes.

Contigs with previously identified gene matches were carried forward for further analysis. Functional groups and pathways encompassing the differentially expressed genes were identified based on GO analysis and pathway analysis based on the Kyoto Encyclopedia of Genes and Genomes (KEGG) database, and manual literature review.

2.6. Gene ontology and enrichment analysis

In order to identify overrepresented GO annotations in the differentially expressed gene set compared to the broader reference assembly, GO analysis and enrichment analysis of significantly expressed GO terms were performed using Ontologizer 2.0 using the Parent–Child–Intersection method with a Benjamini–Hochberg multiple testing correction (Bauer et al., 2008; Grossmann et al., 2007). GO terms for each gene were obtained by utilizing UniProt annotations for the unigene set. The difference of the frequency of assignment of gene ontology terms in the differentially expressed gene sets was compared to the overall striped bass reference assembly. The threshold was set as FDR value < 0.05.

2.7. Experimental validation—QPCR

Fifteen significantly expressed genes with different expression patterns were selected for validation using real time QPCR with gene specific primers designed using Primer3 software. Primers were designed based on contig sequences (Supplementary Table 1). Total RNA (from the same tissue samples as described above) was extracted using the RNeasy Plus Universal Mini Kit (Qiagen) following manufacturer's instructions. RNA samples were DNase treated using the gDNA eliminator solution. First strand cDNA was synthesized by iScript™ cDNA Synthesis Kit (Bio-Rad) according to the manufacturer's protocol. The iScript chemistry uses a blend of oligo-dT and random hexamer primers. All the cDNA products were diluted to 250 ng/μL and utilized for the quantitative real-time PCR reaction using the SsoFast™ EvaGreen® Supermix on a CFX96 real-time PCR Detection System (Bio-Rad Laboratories, Hercules, CA). The thermal cycling profile consisted of an initial denaturation at 95 °C (for 30 s), followed by 40 cycles of denaturation at 94 °C (5 s), and an appropriate annealing/extension temperature (58 °C, 5 s). An additional temperature ramping step was utilized to produce melting curves of the reaction from 65 °C to 95 °C. Results were expressed relative to the expression levels of 18S rRNA in each sample using the Relative Expression Software Tool (REST) version 2009 (Pfaffl et al., 2002). The biological replicate fluorescence intensities of the control and treatment products for each gene, as measured by crossing-point (Ct) values, were compared and converted to fold differences by the relative quantification method. Expression differences between groups were assessed for statistical significance using a randomization test in the REST software. The mRNA expression levels of all samples were normalized to the levels of 18S ribosomal RNA gene in the same samples. Test amplifications were conducted to ensure that 18S and target genes were within an acceptable range. A no-template control was run on all plates. QPCR analysis was repeated in triplicate runs (technical replicates) to confirm expression patterns.

2.8. Mitochondrial bioenergetics and mass

As a means to functionally assess the transcriptomic data, a Seahorse Bioscience XF24 Extracellular Flux Analyzer (Seahorse Biosciences, North Billerica, Massachusetts, USA) was used to measure cellular respiration (oxygen consumption rate; OCR) in freshly isolated liver from

DO25 and DO100 fish (five fish from each treatment). The XF24 instrument detects small changes in oxygen levels within the media immediately surrounding tissue. This is achieved by creating a transient < 10 μL microchamber in which changes in oxygen and pH can be measured non-invasively, sensitively, and repeatedly over time (Ferrick et al., 2008). The OCR was measured for each replicate liver sample in islet plates (Seahorse Biosciences) three times over the course of 15 min and the average OCR was calculated for each treatment. All measurements were then normalized to total protein levels in each well assayed at the completion of the XF24 protocol. Cells were lysed with protein extraction reagent (Pierce/Thermo Scientific, Rockford, IL) and total protein concentrations were determined with the Coomassie Plus (Bradford) Assay Kit (Pierce/Thermo Scientific, Rockford, IL) (Bradford, 1976). Mitochondrial mass was measured by staining liver cells derived from DO25 and DO100 fish (n = 3 fish per treatment) with the targeted fluorescent probe, Mitotracker Red (Invitrogen), followed by fluorescence analysis with a BD Accuri C6 flow cytometer (BD; San Jose, California). This method has been used to determine the mitochondrial mass within eukaryotic cells (Cottet-Rousselle et al., 2011).

3. Results

3.1. Sequencing of short expressed reads from striped bass gill and skin

Illumina-based RNA-sequencing (RNA-seq) was carried out on liver samples from hybrid striped bass. Reads from different samples were distinguished through the use of multiple identifier (MID) tags. A total of 458 million 100 bp high quality reads were generated on an Illumina HiSeq 2000 instrument in a single lane. Greater than 34 million reads were generated for each of the twelve libraries. After removing ambiguous nucleotides, low-quality sequences (quality scores < 20) and short reads (length < 30 bp), the remaining high-quality reads were carried forward for assembly and analysis. Raw read data are archived at the NCBI Sequence Read Archive (SRA) under Accession SRP040452.

3.2. De novo assembly of striped bass liver transcriptome

Trinity generated approximately 179,286 contigs with average length of 1416 bp and N50 size of 2993 bp in its initial assembly, with 72,001 contigs longer than 1000 bp and 100,691 contigs longer than 500 bp (Table 1). Over 77.41% of reads were mapped to the Trinity reference transcriptome.

3.3. Gene identification and annotation

BLAST-based gene identification was performed to annotate the striped bass liver transcriptome and inform downstream differential expression analysis. After gene annotation, 66,932 Trinity contigs had a significant BLAST hit against 19,316 unique UniProt genes (Table 2). 16,695 unigenes were identified based on hits to the UniProt database with the more stringent criteria of a BLAST score ≥ 100 and E-value ≤ 1e−20. The same BLAST criteria were used in comparison of the Trinity reference contigs with the nonredundant (NR) database. The largest number of matches was to the NR database with

Table 1
Summary of de novo assembly results of Illumina sequence data from hybrid striped bass liver using Trinity.

Contigs	179,286
Large contigs (≥ 1000 bp)	72,001
Large contigs (≥ 500 bp)	100,691
N50 (bp)	2993
Average contig length	1416
Reads mapped to final reference (%)	77.41%

Table 2

Summary of gene identification and annotation of assembled striped bass contigs based on BLAST homology searches against various protein databases (UniProt, nr). Putative gene matches were at E-value $\leq 1e-5$. Hypothetical gene matches denote those BLAST hits with uninformative annotation. Quality unigenes hits denote more stringent parameters, including score ≥ 100 , E-value $\leq 1e-20$.

	UniProt	nr
Contigs with putative gene matches	66,932	75,627
Annotated contigs (≥ 500 bp)	60,671	66,307
Annotated contigs (≥ 1000 bp)	53,298	57,047
Unigene matches	19,316	25,532
Hypothetical gene matches	0	2426
Quality unigene matches	16,695	20,852

75,627 contigs with putative gene matches to NR and 20,852 quality unigene matches (Table 2).

3.4. Identification and analysis of differentially expressed genes

Differential expression analysis was performed between 100% DO saturation (DO100 or normoxia) and 25% DO saturation groups (DO25 or chronic hypoxia), between DO100 and DO100 \rightarrow DO25 (acute hypoxia), and between DO25 and DO25 \rightarrow DO100 groups. A total of 1403 unique genes (based on assigned identifiers from the NR database) showed significant differential expression in liver (Fig. 1). In detail, there were 91 differentially expressed genes between DO100 and DO25 saturation groups (Table 3; shown as chronic hypoxia), a meager 39 genes differently expressed between DO25 saturation and DO25 \rightarrow DO100 saturation groups, and the greatest degree of differential expression was observed in DO100 and DO100 \rightarrow DO25 saturation comparison, with 587 up-regulated genes and 752 down-regulated genes (total 1339 genes). Supplementary Table 3 shows all significantly differentially expressed genes for the entire study. Short read coverage within differentially expressed contigs is critical for accurate quantification of expression levels. We obtained good coverage of differentially expressed contigs, with an average of 508 reads per contig.

3.5. Enrichment and pathway analysis

A total of 4374 GO terms including 696 (15.91%) cellular component terms, 1376 (31.46%) molecular functions terms and 2302 (52.63%)

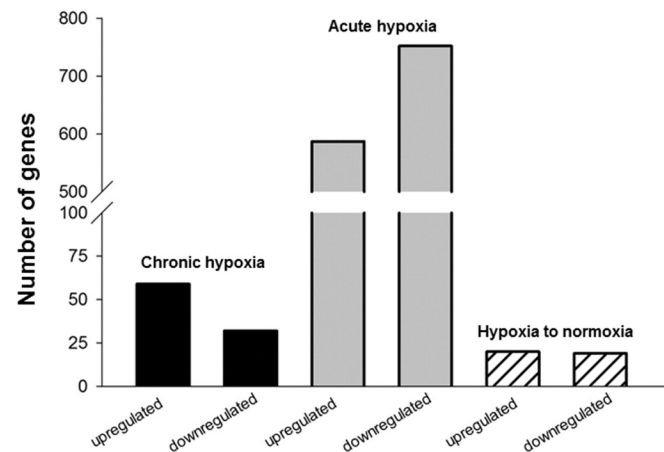


Fig. 1. The number of genes that were statistically differentially expressed under each condition and the direction of their expression. Chronic hypoxia (25% oxygen saturation for 90 days) resulted in transcriptional changes to 91 genes (59 upregulated, 32 downregulated); acute hypoxia (25% oxygen saturation for 6 h) altered 1339 genes (587 upregulated, 752 downregulated), and the movement of fish from the chronic hypoxia treatment to normoxia treatment (100% oxygen saturation) changed 39 genes (20 upregulated, 19 downregulated).

biological process terms were assigned to the 1403 unique gene matches. The percentages of annotated hybrid striped bass sequences assigned to GO terms are shown in Supplementary Fig. 1. The differentially expressed unique genes were then used as inputs to perform enrichment analysis using Ontologizer 2.0. A total of 53 terms with p-value (FDR-corrected) < 0.05 were considered significantly overrepresented. Ten higher level GO terms were retained (the most significant) as informative for further pathway analysis discussion (Table 4).

3.6. Validation of RNA-seq profiles by QPCR

In order to validate the differentially expressed genes identified by RNA-Seq, we selected 15 genes for QPCR confirmation, selecting from those with differing expression patterns and from genes of interest based on functional enrichment and pathway results. Samples from hybrid striped bass (with three replicate sample pools per timepoint) were used for QPCR. Primers were designed based on contig sequences (Supplementary Table 1). Melting-curve analysis revealed a single product for all tested genes. Fold changes from QPCR were compared with the RNA-seq expression analysis results. As shown in Supplementary Table 2 QPCR results were significantly correlated with the RNA-seq results at each timepoint (average correlation coefficient 0.94 for both chronic and acute hypoxia treatments). The majority of examined genes had the same direction (up- or down-regulated) of differential expression by both methods indicating the reliability and accuracy of the Trinity reference assembly and RNA-seq-based transcriptome expression analysis.

3.7. Bioenergetics of liver

Extracellular flux analysis of liver cells obtained from DO100 and DO25 fish revealed significant differences in oxygen consumption rates (OCR), with DO25 liver possessing around 25% higher OCR (Fig. 2A). Mitotracker Red staining of liver cell suspensions from DO25 and DO100 fish showed that DO25 liver cells showed a heightened fluorescence levels, indicative of a greater mitochondrial content (Fig. 2B).

4. Discussion

Next-generation sequencing platforms have propelled rates of discovery, particularly in non-model species where few genomic and transcriptomic resources are available. Work by our group showed previously the phenotypic impacts of chronic hypoxia on hybrid striped bass feeding behavior and growth traits (Green et al., 2015). Here, we delve further into this area to examine the molecular consequences of oxygen deprivation in an effort to reveal the molecular underpinnings responsible for the overall poorer performance under hypoxemia. These studies were performed on whole liver tissue, which is comprised of a number of cell types including blood cells (e.g. erythrocytes), resident and circulating immune cells, hepatocytes, exocrine pancreas, and fibrous connective tissue. The specific contribution of each tissue or cell type to the differential transcriptomic profiles is not known; however, future studies should consider selectively evaluating the effects of hypoxia on cell types of interest by employing techniques such as laser capture microdissection or the use of primary cell lines. Our results indicate that numerous molecular networks were affected by hypoxia, particularly in acute hypoxemia, and that the status of many of these genes returned to basal levels by the time of sampling of fish exposed to chronic hypoxia. Rather than an exhaustive characterization of the fate of every gene differentially regulated, this discussion will highlight the pathways that were predominately disrupted by low oxygen levels; which point towards such processes as lipid utilization, metabolism, and cellular death as being the most affected.

Table 3

Differentially expressed genes in the liver between fish reared under conditions of chronic hypoxia and acute hypoxia versus normoxia. Numbers indicate fold changes relative to normoxia. All of the 91 genes found to be significantly differently expressed between chronic hypoxia and normoxia are shown. The status of these same genes under acute hypoxia is also shown. Positive values indicate higher expression in the hypoxia treatments while negative values indicate higher expression in normoxic fish. Bold values indicate a significant fold change (FDR-corrected $p < 0.05$).

Description	Accession #	Chronic	Acute
Ceruloplasmin	CAL92184.1	4756.71	22,045.56
Ras-related protein Rab-35	XP_003442620.1	1458.42	1801.52
cAMP-specific 3',5'-cyclic phosphodiesterase 4D	XP_003449127.1	1431.75	1582.64
Ephrin type-A receptor 2	XP_003448439.1	1293.37	297.83
RNA-binding protein 5	CBN80582.1	1242.40	1495.51
Ependymin	ABU49423.1	1165.10	582.63
Nuclear receptor subfamily 4 group A member 1	XP_003441554.1	1003.02	213.45
THO complex subunit 5 homolog	XP_003451719.1	955.34	1290.58
S-formylglutathione hydrolase	XP_003449550.1	933.59	1738.32
Triple functional domain protein	XP_003443871.1	778.10	66.75
TBC1 domain family member 17	XP_003442570.1	767.43	887.37
Puromycin-sensitive aminopeptidase	XP_003454172.1	763.94	980.86
Vacuole membrane protein 1	XP_003441662.1	714.42	–1.00
UDP-N-acetylglucosamine–dolichyl-phosphate	XP_003446913.1	685.16	122.62
Connector enhancer of kinase suppressor of ras 2	XP_003453294.1	649.19	293.01
Ankyrin repeat domain-containing protein 50	XP_003454933.1	628.85	–1.00
Plasma membrane calcium-transporting ATPase 3	XP_003447755.1	613.74	172.43
Cytochrome c oxidase subunit 4 isoform 2	P80971.2	582.09	–1.00
Very long-chain specific acyl-CoA dehydrogenase	NP_997776.1	558.45	4322.19
Rho-associated protein kinase 2	XP_003458292.1	551.17	2676.15
Forkhead box protein P1-B	XP_003438999.1	463.67	59.14
Glutamyl-tRNA synthetase	XP_003439051.1	443.57	652.69
Band 4.1 protein 3	XP_003448565.1	431.26	114.73
Dyslexia-associated protein KIAA0319 protein	XP_003447281.1	428.74	45.28
Ribosomal L1 domain-containing protein 1	XP_003438596.1	428.65	3286.79
aarF domain containing kinase 5	NP_001189455.1	419.77	1611.29
Regulating synaptic membrane exocytosis protein 1	XP_003454669.1	382.17	445.34
Butyrophilin subfamily 3 member A3	XP_003457916.1	365.90	271.71
Y-box binding protein	NP_001098143.1	338.43	421.57
RING finger protein 165	XP_003446206.1	314.93	350.47
Guanine nucleotide exchange factor DBS	XP_003451608.1	301.57	82.79
Vesicle-fusing ATPase	CBN81692.1	298.93	275.45
Urea transporter 2	XP_003451724.1	276.85	29.61
CB055 protein	NP_001158878.1	264.60	306.15
Paxillin	XP_003441455.1	253.28	218.07
Uridine phosphorylase 1	XP_003454505.1	238.65	340.44
F-box/WD repeat-containing protein TBL1XR1	XP_003444342.1	237.69	119.32
RING finger protein 222	XP_003458916.1	215.29	3.98
Polyadenylate-binding protein nuclear 1 isoform 1	NP_998424.1	191.85	151.31
Probable palmitoyltransferase ZDHHC6	CBN81489.1	186.95	–1.00
Autophagy-related protein 13	XP_003455930.1	173.45	855.42
Heme oxygenase-	XP_003443134.1	169.19	189.60
Class E basic helix–loop–helix protein 41	XP_003440406.1	128.35	35.37
Stromal interaction molecule 1	XP_003455987.1	120.18	86.86
Cyclic AMP-dependent transcription factor ATF-3	XP_003446694.1	75.23	9.08
Transcriptional regulator Myc-B	XP_003459605.1	69.06	34.49
Ras-GEF domain-containing family member 1B-B	XP_003444479.1	44.57	6.71
Low quality protein:	XP_003455749.1	41.57	20.71
Alpha-actinin-1 isoform 2	XP_003445507.1	35.97	12.63
Leukocyte immune-type receptor 3 precursor	NP_001187136.1	32.66	–30.15
Cyclin-dependent kinase inhibitor 1C	XP_003443975.1	30.45	36.34
GTP-binding protein Rhes	XP_003447949.1	19.85	7.66
Heme oxygenase 1	ABL74501.1	18.99	47.74
Butyrophilin subfamily 1 member A1 precursor	ACN10676.1	17.84	4.02
Ornithine decarboxylase	XP_003445497.1	16.07	74.54
Protein PRRC2B	XP_003455022.1	15.48	12.88
Palladin	XP_003439820.1	15.05	17.49
Zinc finger CCH domain-containing protein 11A	CBN80943.1	13.69	11.73
Phosphoenolpyruvate carboxykinase	ADB66756.1	12.07	282.40
Vitamin D 25-hydroxylase	XP_003442430.1	–14.68	–22.07
14-3-3 protein beta/alpha-2	NP_001133672.1	–19.48	1.75
Nitrogen permease regulator 3 protein	XP_003442244.1	–20.69	–2.26
ETS-related transcription factor ELF-2	XP_003448064.1	–42.19	9.86
Sodium-coupled neutral amino acid transporter	XP_003453134.1	–175.34	2.32
Sulfate anion transporter 1	XP_003444477.1	–186.36	–3.08
Coiled-coil domain-containing protein 5	XP_003446448.1	–218.08	1.22
Upstream-binding protein 1	XP_003444097.1	–231.60	–1.05
Polyphosphoinositide phosphatase	XP_003449893.1	–240.50	1.32
Rho guanine nucleotide exchange factor 11	XP_003458910.1	–244.33	–247.64
Protein NLRCS	NP_001186995.1	–244.68	–1.55
Ubiquitin carboxyl-terminal hydrolase 2	XP_003453780.1	–247.90	–1.06

(continued on next page)

Table 3 (continued)

Description	Accession #	Chronic	Acute
Multidrug resistance-associated protein 1	XP_003456926.1	–253.70	–2.65
Calcitonin receptor 1	BAE45312.1	–268.35	–3.37
Vacuolar protein sorting-associated protein 13C	XP_003437776.1	–271.62	–1.41
Zinc finger protein 644	XP_003438073.1	–298.17	–302.21
Probable histone deacetylase 1-B	XP_003443815.1	–308.84	1.58
Atrial natriuretic peptide receptor 1	XP_003443830.1	–315.71	–1.75
Autism susceptibility gene 2 protein	CBN81719.1	–338.08	–1.98
SH3 and PX domain-containing protein 2 A	XP_003454685.1	–365.93	–3.76
Monocyte to macrophage differentiation factor 2	XP_003443179.1	–444.84	1.69
Vitamin D3 receptor A	XP_003449167.1	–445.75	–3.63
Proactivator polypeptide isoform 1	XP_003441060.1	–454.55	1.12
Phosphatidylserine synthase 2	XP_003443888.1	–588.58	1.31
Exostosin-1b	XP_003447212.1	–592.79	–4.15
AF017303_1 FMVIA	AAD52005.1	–723.36	–1.72
Ubiquitin domain-containing protein UBFD1	XP_003442107.1	–747.29	1.68
Acetyl-coenzyme A synthetase, cytoplasmic	XP_003444850.1	–751.55	–4.70
Platelet-derived growth factor receptor beta a	ABD48800.1	–1007.08	–1.20
myb-binding protein 1A protein	XP_003451480.1	–1837.67	–2.49
Histone-lysine N-methyltransferase MLL3	XP_003437952.1	–1969.23	–2.21
Elastase 4 precursor	ACM41852.1	–267,767	–271,402

Table 4

Summary of GO term enrichment result of expressed genes in hybrid striped bass after hypoxia. The 1403 (overall, A), 1339 (acute, B), and 91 (chronic, C) differentially expressed genes were analyzed as the study set in comparison to all unigenes. FDR \leq 0.05 was considered significant. Population count is the number of genes associated with the term in the population set (all genes). Study count is the number of genes associated with the term in the study set (the significantly differentially expressed genes). GO names were retained only from GO terms of levels > 2.

GO ID	GO name	p-Value (FDR)	Population count	Study count
A				
GO:0006629	Lipid metabolic process	0.0069	118	18
GO:006082	Organic acid metabolic process	0.0429	135	16
GO:0008219	Cell death	0.0100	118	16
GO:0016265	Death	0.0215	118	16
GO:0044255	Cellular lipid metabolic process	0.0498	82	11
GO:0009719	Response to endogenous stimulus	0.0159	58	10
GO:0010941	Regulation of cell death	0.0084	61	10
GO:0006869	Lipid transport	0.0044	29	7
GO:0009055	Electron carrier activity	0.0273	38	7
GO:0060548	Negative regulation of cell death	0.0100	30	7
B				
GO:0006629	Lipid metabolic process	0.0096	118	17
GO:0008219	Cell death	0.0120	118	15
GO:0010941	Regulation of cell death	0.0052	61	10
GO:0005102	Receptor binding	0.0066	73	10
GO:0014070	Response to organic cyclic compound	0.0097	34	8
GO:0006869	Lipid transport	0.0029	29	7
GO:0060548	Negative regulation of cell death	0.0075	30	7
GO:0010876	Lipid localization	0.0121	31	7
GO:0030522	Intracellular receptor signaling pathway	0.0047	23	6
GO:0097373	MCM complex	0.0055	8	3
C				
GO:0004872	Receptor activity	0.0173	150	4
GO:0060089	Molecular transducer activity	0.0342	184	4
GO:0070887	Cellular response to chemical stimulus	0.0200	91	3
GO:0022610	Biological adhesion	0.0209	98	3
GO:0022607	Cellular component assembly	0.0246	115	3
GO:0005975	Carbohydrate metabolic process	0.0259	113	3
GO:0007155	Cell adhesion	0.0311	98	3
GO:0044085	Cellular component biogenesis	0.0478	144	3
GO:0019199	Transmembrane receptor protein kinase activity	0.0251	21	2
GO:0004713	Protein tyrosine kinase activity	0.0499	31	2

4.1. Fatty acid metabolism

Previously (using the same experimental cohorts of the fish employed here), we observed significantly larger livers (as indicated by the hepatosomatic index) in HSB reared in normoxia versus hypoxia and reported significantly higher levels of whole body lipid (Green et al., 2015). Qualitatively, the enlarged livers were noticeably pale and soft in texture, while fish exposed to hypoxia exhibited livers that were darkened in appearance, firm, and friable (Green et al., 2015). These observations led us to focus on examining the liver transcriptome in the present study. Indeed, the liver plays a central role in metabolic homeostasis, and is a major site for the synthesis, metabolism, storage and redistribution of processed carbohydrates, proteins and lipids (Bechmann et al., 2012). In tissues such as the heart and liver, lipids provide a rich source of energy via oxidative phosphorylation by mitochondria (Jungermann, 1988; Shohet and Garcia, 2007). In mammals, where hypoxic stress is typically viewed as a pathological state (e.g., fatty liver disease, ischemia), lipid metabolism under low oxygen conditions is reprogrammed to suppress mitochondrial oxidation of lipids as a protective measure against toxic metabolites and oxidative stress. Broadly, hypoxia promotes lipid storage and inhibits lipid catabolism through β oxidation (Whitmer et al., 1978; Bostrom et al., 2006). In contrast, in aquatic animals, environmental hypoxia is a common challenge that many aquatic organisms experience in their habitat and responding to hypoxia requires metabolic reprogramming so that energy-demanding processes are regulated to match available energy reserves (Gracey et al., 2011). Gene expression data in the hypoxia-tolerant burrow-dwelling goby, *Gillichthys mirabilis*, revealed that pathways associated with triglyceride hydrolysis were upregulated by hypoxia whereas pathways associated with triglyceride synthesis were downregulated (Gracey et al., 2011). Recently, in common carp *Cyprinus carpio*, exposure to chronic hypoxia was shown to increase lipid peroxidation within the liver (Mustafa et al., 2015). Here, we observed changes—with similarities and differences to work in mammals and other teleosts—in multiple genes involved in lipid catabolism and β oxidation, particularly following acute hypoxia. Long-chain fatty acid-CoA ligase 4 (FACL4) is an essential enzyme in fatty acid metabolism and in mammals it controls the level of free arachidonic acid (ARA), which is a key regulatory point in the generation of lipid mediators (Kang et al., 1997). Compared to fish held in normoxia, FACL4 was significantly down-regulated 972-fold in acute hypoxia; which, while not measured directly, could have resulted in heightened ARA levels. Exogenous ARA administration has been shown to exert beneficial effects on hepatic hemodynamics and cellular integrity under conditions

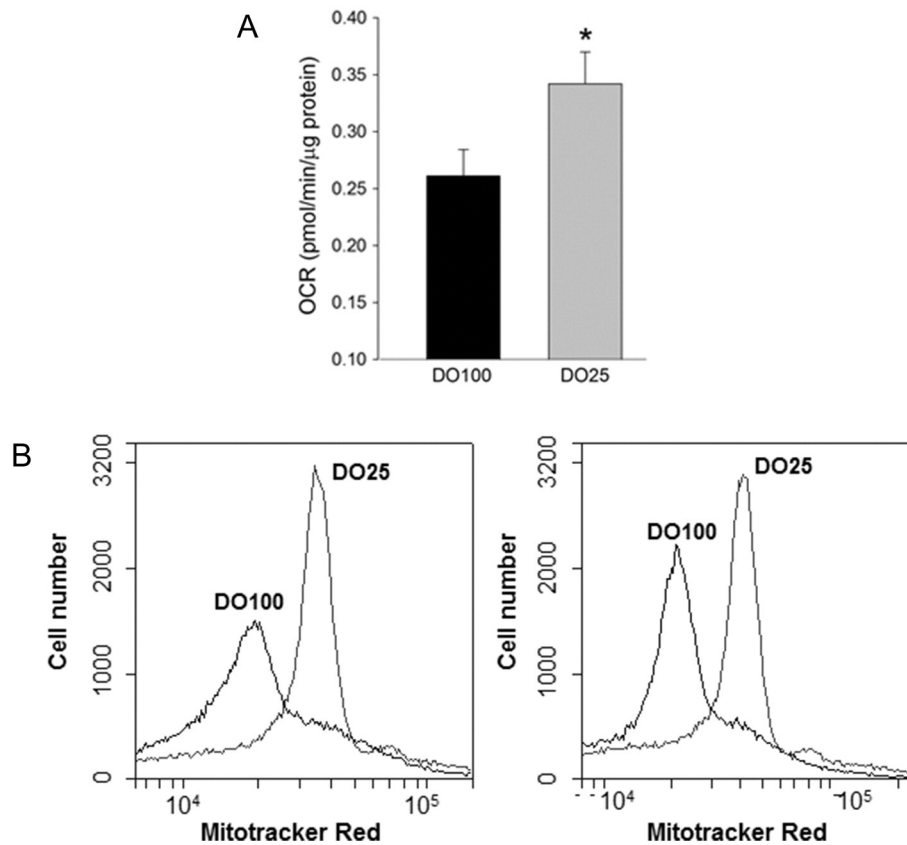


Fig 2. A.) Liver tissue isolated from fish subjected to chronic hypoxia show greater oxygen consumption rates (OCR; mean \pm SEM; five fish per treatment) and B.) increased mitochondrial content (two representative fish from each treatment) as indicated by the fluorescence intensity derived from staining with the mitochondrion-selective dye Mitotracker Red.

of hypoxia in mammals (Flynn, 1979). In sturgeon, supplementation of a standard ration with higher PUFA levels and Vitamin E led to improved tolerance to hypoxia (Randall et al., 1992). While the exact dietary link was not established, the fish fed the PUFA + Vitamin E ration were shown to have higher ARA levels in their tissues (Randall et al., 1992). Supplementation of ARA in the context of aquaculture feeds is gaining increasing attention, and was recently explored in the closely related European sea bass where ARA inclusion was shown to protect against handling stress (Atalah et al., 2011). Studies should examine whether protection against hypoxia could be obtained with diets featuring greater ARA inclusion rates; a breakthrough that would offer huge benefits in the captive rearing of hybrid bass and other related warmwater finfish.

The current knowledge on lipoprotein metabolism is based on many different biochemical and metabolic studies which will be briefly summarized (see review by Beisiegel, 1998). Exogenous fat is transported in chylomicrons from the intestine to the liver. After entry in the blood stream the chylomicrons are hydrolyzed by the endothelial-bound lipoprotein lipase. The chylomicron remnants are rapidly taken up by the liver via the low-density lipoprotein receptor (LDLR) and the low-density lipoprotein receptor-related protein 1 (LRP1). Apolipoprotein E (APOE) and lipoprotein lipase are the recognition signals for these receptors. Under maintenance conditions, the interaction between LRP1 and APOE stimulates a signaling pathway that leads to elevated intracellular cyclic-AMP (cAMP) levels as well as increased protein kinase A (PKA) activity, thus triggering endocytosis or other intracellular signaling (Goretzki and Mueller, 1997; Li et al., 2001). In the current study, acute hypoxia resulted in the downregulation of LDLR and LRP1 490-fold and 4500-fold respectively, while APOE was upregulated 5-fold and PKA was downregulated nearly 10-fold. The significant downregulation of LDLR, LRP1, as well as PKA could point to lower levels of cellular endocytosis of ligands, both lipid and non-lipid in nature,

and/or attenuated intracellular signaling, both processes which are cAMP-dependent and therefore energetically expensive. This is further evident by the fact that adenylate cyclase, the protein that converts ATP to cAMP was also significantly downregulated (-28 -fold) in fish exposed to acute hypoxia.

Relatedly, lipid phosphate phosphohydrolase 1 (LPP1) plays an important physiological role in controlling the degradation of circulating lysophosphatidic acid (LPA), a lipid mediator that stimulates cell proliferation and growth; particularly the growth of new blood vessels, a process termed angiogenesis. Reduced LPP1 expression (-11.5 -fold), as observed in fish subjected to acute hypoxia, could allow for higher circulating levels of LPA, which could offer protection against hypoxia-induced damage (as evidenced by its cardioprotective role in mammals) or drive angiogenic processes within tissues in need of improved oxygen delivery (Tomsig et al., 2009; Karlner et al., 2001). The importance of LPA in the HSB hepatic response to acute hypoxia is further supported by the upregulation of LPA receptor 3 ($+335$ -fold) and LPA phosphatase type 6 ($+9$ -fold), both of which are involved in the hydrolysis of LPAs (Contos et al., 2000; Tigyi & Parrill, 2003), and lipase member H ($+4$ -fold) which catalyzes the production of LPAs (Sonoda et al., 2002). The precise interplay and functional significance between these and other pathway members related to lipid metabolism and storage is unclear at this point and our findings do not always precisely correlate with the paradigms described in mammals. Some of the changes could also be species-specific, or related to the severity of hypoxia. Specifically, no mortality occurred in either the acute or chronic hypoxia treatment; thus it stands to reason that the transcriptomic profiles reported here could be different under conditions approaching more sublethal to lethal oxygen levels. Nevertheless, it is apparent that the liver is markedly affected by oxygen levels, to the point that liver growth/size is impaired and that these differential expression signatures offer some insight into the mechanism.

4.2. Regulation of cell death

Maintenance of whole animal-level homeostasis hinges upon the coordinated regulation of cellular proliferation and death across the range of host tissues. Enrichment analysis pointed us towards a deeper examination of cell death processes. Two pathways related to cellular preservation, apoptosis and autophagy, were clearly influenced by hypoxic insult. Apoptosis is characterized by cell shrinkage, chromatin condensation, internucleosomal DNA cleavage, membrane blebbing, and the formation of apoptotic bodies that are phagocytosed by other cells (García-Domingo et al., 2003). Apoptosis is a stepwise cascade of events principally orchestrated by proteases termed caspases. Immediately apparent was the complete lack of caspase induction in any treatment. Instead, a variety of substantial transcriptional changes related to the suppression of apoptosis were induced, particularly in acute hypoxic fish. The Death-inducer obliterator 1 (DIDO1 or DIO-1) gene has been shown to be a key mediator of apoptosis in mammalian models. Overexpression of DIDO1 in cultured cells strongly activates apoptotic machinery to induce apoptosis; however, apoptosis is blocked by the addition of caspase inhibitors or by BCL-2 overexpression (García-Domingo et al., 1999; García-Domingo et al., 2003). Accordingly, in the present study, DIDO-1 was downregulated nearly 500-fold in acute hypoxia and concomitantly, the hallmark anti-apoptotic factor BCL-2 was upregulated over 4-fold. Similarly, Bcl-2-related ovarian killer protein (BOK), a potent pro-apoptotic factor, was downregulated over 300 fold in acute hypoxia fish. Further, the trademark apoptotic effector, tumor necrosis factor-related apoptosis-inducing ligand (TRAIL), which is a member of the tumor necrosis factor (TNF) family of ligands and a potent inducer of apoptosis, was significantly downregulated over 4 fold in acute hypoxia fish. The microenvironment of tumors commonly features a hypoxic core; thus numerous studies have highlighted that hypoxia can protect malignantly transformed cells from TRAIL-mediated apoptosis. However, we found no previous evidence in the human, murine, or teleost situation showing that hypoxia can suppress TRAIL expression as reported herein. Collectively, it appears that hybrid striped bass hepatic responses feature a broad suppression of transcripts of pro-apoptotic factors. Presumably, this type of response would offer protection not only against hepatocellular damage, but more widespread organismal damage or even death.

Aside from apoptosis, several genes related to autophagy were differentially expressed in both chronic and acute hypoxic conditions. Autophagy is an important catabolic process that refers exclusively to those pathways that lead to the elimination of cytoplasmic components by their delivery to lysosomes, where metabolites are then salvaged and reused either as energy sources or as building blocks for the synthesis of new macromolecules (Boya et al., 2013). While perhaps best studied in the context of nutrient deprivation, the induction of autophagy by hypoxia is a growing area of interest, namely in the biomedical sciences. Obvious interplay between autophagy and apoptosis has been documented in the mammalian literature; however little is known about the coordination of these two processes in fish. Generally speaking, autophagy blocks the induction of apoptosis and inhibits the activation of apoptosis-associated caspases which could reduce cellular injury (Li et al., 2015). The autophagy-related proteins 4B, 4D, 13 and 15 were strongly upregulated, particularly in DO25 fish. Autophagy is known to induce cell cycle arrest via downstream effects on translation of key cell cycle genes, such as cyclins (Glick et al., 2010). Several cyclin-dependent kinases were downregulated in DO25 animals, which could have broadly inhibited cell cycle progression within hepatocytes or other cell populations comprising the liver. In taking together the gross differences in liver size, the alterations in lipid utilization, the suppression of apoptosis combined with the induction of autophagy, our findings suggest that the hepatic tissue of hybrid striped bass may have entered a state of senescence. This may have allowed the animals to liberate, redirect, or shunt resources to other vital tissues to survive hypoxia.

4.3. Functional validation study

The use of RNA-seq allows for the examination of global transcriptional changes in a tissue at a particular snapshot in time. However, it is widely understood that the level of transcriptional message does not always correlate with protein. With little to no resources (i.e., antibodies) available for HSB, we utilized extracellular flux analysis to quantify aerobic respiration in liver tissue obtained from DO100 and DO25 fish. Unexpectedly, under conditions of reduced oxygen availability, liver cells from DO25 fish showed significant increases in basal oxygen consumption rates; a surrogate measure of mitochondrial function. Curiously, as compared to our previous work with established fish cell lines (Beck and Fuller, 2012), total aerobic respiration was lower and glycolysis was virtually non-detectable (not shown). Further optimization may be needed, namely in media composition or tonicity, to allow for long-term repeated measuring of primary liver cells isolated from HSB. By using a fluorophore that selectively stains mitochondria, we documented an increase in the mass (linked to number/size of mitochondria) of the mitochondrial compartment, which could have accounted for the increase in oxygen consumption by DO25 liver cells. An increase in mitochondrial number, a process termed mitochondrial biogenesis, is a common cellular response to hypoxia and is thought to improve the efficiency of oxygen consumption and ATP synthesis, and in parallel counteract potential cellular damage brought about by hypoxia (Kopp et al., 2014). Similar to our present findings, an increase in mitochondrial content has been observed in larval zebrafish subjected to hypoxia (Kopp et al., 2014). Consistent with these observations is a greater than 400 fold increase in PGC-1 β message in liver tissue from the acute hypoxia treatment. In contrast to mammals, where PGC-1 α is regarded as the archetypal master regulator of mitochondrial biogenesis, recent evidence from teleosts suggests that PGC-1 β may exert more control over mitochondrial gene expression (LeMoine et al., 2008). Intriguingly, and related to the above discussion on lipid metabolism, PGC-1 β is also known to play a key regulatory role in hepatic lipid metabolism with PGC-1 β knockout mice being more susceptible to hepatic steatosis (Sonoda et al., 2007) and the transduction of rodent liver with PGC-1 β decreased hepatic lipid while plasma triglyceride and cholesterol levels were significantly elevated (Lin et al., 2005). Clearly, further research is needed to better understand the interactions between mitochondrial abundance, regulation, and lipid metabolism in hypoxic teleosts. As a step towards clarification, borrowing from biomedical models, future efforts should consider engineering HSB hepatic cells to either grossly overexpress select aforementioned targets of interest, or to silence those same targets, and examine the functional consequences.

Supplementary data to this article can be found online at <http://dx.doi.org/10.1016/j.cbd.2016.01.005>.

Acknowledgments

Special thanks to Greg O'Neal, Matt Barnett, and Matt McEntire for their technical assistance during this study. Mention of trade names or commercial products in this article is solely for the purpose of providing specific information and does not imply recommendation or endorsement by the U.S. Department of Agriculture.

References

- Atalah, E., Hernández-Cruz, C.M., Ganuza, E., Benítez-Santana, T., Ganga, R., Roo, J., Montero, D., Izquierdo, M., 2011. Importance of dietary arachidonic acid for the growth, survival and stress resistance of larval European sea bass (*Dicentrarchus labrax*) fed high dietary docosahexaenoic and eicosapentaenoic acids. *Aquac. Res.* 42, 1261–1268.
- Bacon, N.C., Wappner, P., O'Rourke, J.F., Bartlett, S.M., Shilo, B., Pugh, C.W., Ratcliffe, P.J., 1998. Regulation of the *Drosophila* bHLH-PAS protein Sima by hypoxia: functional evidence for homology with mammalian HIF-1. *Biochem. Biophys. Res. Commun.* 249, 811–816.

- Bauer, S., Grossmann, S., Vingron, M., Robinson, P.N., 2008. Ontologizer 2.0—a multifunctional tool for GO term enrichment analysis and data exploration. *Bioinformatics* 24, 1650–1651.
- Bechmann, L.P., Hannivoort, R.A., Gerken, G., Hotamisligil, G.S., Trauner, M., Canbay, A., 2012. The interaction of hepatic lipid and glucose metabolism in liver diseases. *J. Hepatol.* 56, 952–964.
- Beck, B.H., Fuller, S.A., 2012. The impact of mitochondrial and thermal stress on the bioenergetics and reserve respiratory capacity of fish cell lines. *J. Aquat. Anim. Health* 24, 244–250.
- Beisiegel, U., 1998. Lipoprotein metabolism. *Eur Heart J.* 19 (Suppl. A) A20–3.
- Bostrom, P., Magnusson, B., Svensson, P., Wiklund, O., Boren, J., Carlsson, L.M.S., Stahlman, M., Olofsson, S., Hulten, L.M., 2006. Hypoxia converts human macrophages into triglyceride-loaded foam cells. *Arterioscler. Thromb. Vasc. Biol.* 26, 1871–1876.
- Boya, P., Reggiori, F., Codogno, P., 2013. Emerging regulation and functions of autophagy. *Nat. Cell Biol.* 15, 713–720.
- Bradford, M.M., 1976. A rapid and sensitive method for the quantitation of microgram quantities of protein utilizing the principle of protein–dye binding. *Anal. Biochem.* 72, 248–254.
- Burggren, W.W., 1982. “Air gulping” improves blood oxygen transport during aquatic hypoxia in the goldfish *Carassius auratus*. *Physiol. Zool.* 55, 327–334.
- Contos, J.J.A., Ishii, I., Chun, J., 2000. Lysophosphatidic acid receptors. *Mol. Pharmacol.* 58, 1188–1196.
- Cottet-Rousselle, C., Ronot, X., Leverve, X., Mayol, J.F., 2011. Cytometric assessment of mitochondria using fluorescent probes. *Cytometry A* 79, 405–425.
- Coutant, C.C., 1985. Striped bass, temperature, and dissolved oxygen: a speculative hypothesis for environmental risk. *Trans. Am. Fish. Soc.* 114, 31–61.
- Diaz, R.J., 2001. Overview of hypoxia around the world. *J. Environ. Qual.* 30, 275–281.
- Douglas, D.R., Jahn, L.A., 1987. Radiotracking hybrid striped bass in Spring Lake, Illinois, to determine temperature and oxygen preferences. *North Am. J. Fish Manage* 7, 531–534.
- Ferrick, D., Wu, M., Swift, A., Neilson, A., 2008. Mitochondrial dysfunction assessed quantitatively in real time by measuring the extracellular flux of oxygen and protons. *Drug-Induced Mitochondrial Dysfunction*, pp. 373–382.
- Flynn, J.T., 1979. Influence of the arachidonic acid cascade on the in vitro hepatic response to hypoxia. *Prostaglandins* 17, 39–52.
- García-Domingo, D., Leonardo, E., Grandiën, A., Martínez, P., Albar, J.P., Izpisua-Belmonte, J.C., Martínez-A, C., 1999. DIO-1 is a gene involved in onset of apoptosis in vitro, whose misexpression disrupts limb development. *Proc. Natl. Acad. Sci. U. S. A.* 96, 7992–7997.
- García-Domingo, D., Ramírez, D., de Buitrago, G.G., A.C., M., 2003. Death inducer-oblierator 1 triggers apoptosis after nuclear translocation and caspase upregulation. *Mol. Cell Biol.* 23, 3216–3225.
- Glick, D., Barth, S., Macleod, K.F., 2010. Autophagy: cellular and molecular mechanisms. *J. Pathol.* 221, 3–12.
- Goretzki, L., Mueller, B.M., 1997. Receptor-mediated endocytosis of urokinase-type plasminogen activator is regulated by cAMP-dependent protein kinase. *J. Cell Sci.* 110, 1395–1402.
- Grabherr, M.G., Haas, B.J., Yassour, M., Levin, J.Z., Thompson, D.A., Amit, I., Adiconis, X., Fan, L., Raychowdhury, R., Zeng, Q., 2011. Full-length transcriptome assembly from RNA-Seq data without a reference genome. *Nat. Biotechnol.* 29, 644–652.
- Gracey, A.Y., Lee, T.H., Higashi, R.M., Fan, T., 2011. Hypoxia-induced mobilization of stored triglycerides in the euryoxic goby *Gillichthys mirabilis*. *J. Exp. Biol.* 214, 3005–3012.
- Green, B.W., Rawles, S.D., Fuller, S.A., Beck, B.H., McEntire, M.E., 2015. Hypoxia affects performance traits and body composition of juvenile hybrid striped bass (*Morone chrysops* × *M. saxatilis*). *Aquacult. Res.* <http://dx.doi.org/10.1111/are.12678>.
- Grossmann, S., Bauer, S., Robinson, P.N., Vingron, M., 2007. Improved detection of overrepresentation of Gene-Ontology annotations with parent–child analysis. *Bioinformatics* 23, 3024–3031.
- Gotz, S., Garcia-Gomez, J.M., Terol, J., Williams, T.D., Nagaraj, S.H., Nueda, M.J., Robles, M., Talon, M., Dopazo, J., Conesa, A., 2008. High-throughput functional annotation and data mining with the Blast2GO suite. *Nucleic Acids Res.* 36, 3420–3435.
- Hochachka, P.W., 1986. Defence strategies against hypoxia and hypothermia. *Science* 231, 234–241.
- Jiang, H., Guo, R., Powell-Coffman, J.A., 2001. The *Caenorhabditis elegans* hif-1 gene encodes a bHLH-PAS protein that is required for adaptation to hypoxia. *Proc. Natl. Acad. Sci. USA* 98, 7916–7921.
- Jungermann, K., 1988. Metabolic zonation of liver parenchyma. *Semin. Liver Dis.* 8, 329–341.
- Kang, M.J., Fujino, T., Sasano, H., Minekura, H., Yabuki, N., Nagura, H., Iijima, H., Yamamoto, T.T., 1997. A novel arachidonate-preferring acyl-CoA synthetase is present in steroidogenic cells of the rat adrenal, ovary, and testis. *Proc. Natl. Acad. Sci. U. S. A.* 94, 2880–2884.
- Karlner, J.S., Honbo, N., Summers, K., Gray, M.O., Goetzl, E.J., 2001. The lysophospholipids sphingosine-1-phosphate and lysophosphatidic acid enhance survival during hypoxia in neonatal rat cardiac myocytes. *J. Mol. Cell. Cardiol.* 33, 1713–1717.
- Kopp, R., Bauer, I., Ramalingam, A., Egg, M., Schwerte, T., 2014. Prolonged hypoxia increases survival even in zebrafish (*Danio rerio*) showing cardiac arrhythmia. *PLoS One* 9 (2).
- LeMoine, C.M., Genge, C.E., Moyes, C.D., 2008. Role of the PGC-1 family in the metabolic adaptation of goldfish to diet and temperature. *J. Exp. Biol.* 211, 1448–1455.
- Li, M., Tan, J., Miao, Y., Lei, P., Zhang, Q., 2015. The dual role of autophagy under hypoxia— involvement of interaction between autophagy and apoptosis. *Apoptosis* 20, 769–777.
- Li, C., Beck, B.H., Fuller, S.A., Peatman, E., 2014. Transcriptome annotation and SNP discovery in white bass (*Morone chrysops*) and striped bass (*Morone saxatilis*). *Anim. Genet.* 45, 885–887.
- Li, Y., van Kerkhof, P., Marzolo, M.P., Strous, G.J., Bu, G., 2001. Identification of a major cyclic AMP-dependent protein kinase A phosphorylation site within the cytoplasmic tail of the low-density lipoprotein receptor-related protein: implication for receptor-mediated endocytosis. *Mol. Cell Biol.* 21, 1185–1195.
- Lin, J., Yang, R., Tarr, P.T., Wu, P.H., Handschin, C., Li, S., Yang, W., Pei, L., Uldry, M., Tontonoz, P., Newgard, C.B., Spiegelman, B.M., 2005. Hyperlipidemic effects of dietary saturated fats mediated through PGC-1 β coactivation of SREBP. *Cell* 120, 261–273.
- Mustafa, S.A., Karieb, S.S., Davies, S.J., Jha, A.N., 2015. Assessment of oxidative damage to DNA, transcriptional expression of key genes, lipid peroxidation and histopathological changes in carp *Cyprinus carpio* L. following exposure to chronic hypoxic and subsequent recovery in normoxic conditions. *Mutagenesis* 30 (1), 107–116.
- Nikinmaa, M., Rees, B.B., 2005. Oxygen-dependent gene expression in fishes. *Am. J. Physiol. Regul. Integr. Comp. Physiol.* 288, R1079–R1090.
- Pfaffl, M.W., Horgan, G.W., Dempfle, L., 2002. Relative expression software tool (REST C) for group-wise comparison and statistical analysis of relative expression results in real-time PCR. *Nucleic Acids Res.* 30, e36.
- Randall, D.J., McKenzie, D.J., Abrami, G., Bondiolotti, G.P., Natiello, F., Bronzi, P., Bolis, L., Agradi, E., 1992. Effects of diet on responses to hypoxia in sturgeon (*Acipenser naccarii*). *J. Exp. Biol.* 170, 113–125.
- Reading, B.J., Chapman, R.W., Schaff, J.E., Scholl, E.H., Opperman, C.H., Sullivan, C.V., 2012. An ovary transcriptome for all maturational stages of the striped bass (*Morone saxatilis*), a highly advanced perciform fish. *BMC Res. Notes* 5, 111.
- Shohet, R., Garcia, J., 2007. Keeping the engine primed: HIF factors as key regulators of cardiac metabolism and angiogenesis during ischemia. *J. Mol. Med.* 85, 1309–1315.
- Sonoda, H., Aoki, J., Hiramatsu, T., Ishida, M., Bandoh, K., Nagai, Y., Taguchi, R., Inoue, K., Arai, H., 2002. A novel phosphatidic acid-selective phospholipase A1 that produces lysophosphatidic acid. *J. Biol. Chem.* 277, 34254–34263.
- Sonoda, J., Mehl, I.R., Chong, L.W., Nofsinger, R.R., Evans, R.M., 2007. PGC-1 β controls mitochondrial metabolism to modulate circadian activity, adaptive thermogenesis, and hepatic steatosis. *Proc. Natl. Acad. Sci.* 104 (12), 5223–5228.
- Tigyi, G., Parrill, A.L., 2003. Molecular mechanisms of lysophosphatidic acid action. *Prog. Lipid Res.* 42 (6), 498–526.
- Tomsig, J., Snyder, A., Berdyshev, E., Skobeleva, A., Mataya, C., Natarajan, V., Brindley, D., Lynch, K., 2009. Lipid phosphate phosphohydrolase type 1 (LPP1) degrades extracellular lysophosphatidic acid in vivo. *Biochem. J.* 419, 611–618.
- Ton, C., Stamatiou, D., Liew, C.C., 2003. Gene expression profile of zebrafish exposed to hypoxia during development. *Physiol. Genomics* 13, 97–106.
- Whitmer, J.T., Idell-Wenger, J.A., Rovetto, M.J., Neely, J.R., 1978. Control of fatty acid metabolism in ischemic and hypoxic hearts. *J. Biol. Chem.* 253, 4305–4309.
- Wu, R.S., Zhou, B.S., Randall, D.J., Woo, N.Y., Lam, P.K., 2003. Aquatic hypoxia is an disrupter and impairs fish reproduction. *Environ. Sci. Technol.* 37, 1137–1141.